Effect of reversible phase-transformations on crack-growth

Stam, G.; van der Giessen, E.

Published in:
Mechanics of Materials

DOI:
10.1016/0167-6636(94)00074-3

Publication date:
1995

ELSEVIER

Mechanics of Materials 21 (1995) 51–71

MECHANICS OF MATERIALS

Effect of reversible phase transformations on crack growth

Geert Stam, Erik van der Giessen

Delft University of Technology, Laboratory for Engineering Mechanics, Delft, The Netherlands

Received 3 August 1994; revised version received 27 October 1994

Abstract

In this work, the influence of partial or full reversibility of a stress-induced phase transformation is investigated, both in terms of the size and shape of the transformation zone around the crack tip, and the toughness development during crack growth. The constitutive equations adopted in this study are due to Sun et al. (1991, *J. Mech. Phys. Solids 39*, 507) and account for transformation-induced dilatant and shear strains. These constitutive equations were designed to model the phase transformations occurring in zirconia ceramics or in shape memory alloys (SMA). The results are obtained by a full field finite element analysis of crack propagation under small scale transformation conditions. The phase transformations considered here tend to give rise to a substantial toughening of the material if the transformation were irreversible. It is shown here that in some cases, the reversibility of the transformation can significantly reduce the toughness increase. A parameter study establishes the sensitivity of this deterioration to characteristics of the constitutive response.

Keywords: Ceramics; Phase transformations; Transformation toughening; Zirconia; Shape memory alloys

1. Introduction

A certain class of solid materials exhibits stress-induced martensitic-type phase transformations. These phase transformations are found in certain metal alloys, called shape memory alloys (SMA) (e.g. Cu–Zn–Sn or Cu–Zn–Al), but also in ceramics comprising or containing tetragonal zirconia. The parent (p) crystal structure transforms to the martensitic phase (m), $p \rightarrow m$, when a certain critical stress level is reached. In fact, a certain incubation time will be necessary for the transformation to start, but this is only in the order of hundreds of nanoseconds (Sano et al., 1992). Once the transformation has initiated, it will typically proceed throughout the crystal lattice with the speed of sound. For quasi-static loading conditions, which we shall focus on here, we may therefore assume that the transformation within a crystal occurs instantaneously and is time independent. However, the crystal lattice has finite dimensions and the boundaries are usually formed by the grain boundaries, while in some cases more than one crystal structure can exist in a single grain. The newly formed crystal structure has different lattice parameters and therefore the transformation involves the development of so-called transformation strains from which the material inherits special properties.

Overviews of the thermoelastic, pseudoelastic and shape memory effects associated with the martensitic transformation of SMA materials are given in the reviews by Delaey et al. (1974), Krishnan et al. (1974) and Warlimont et al. (1974). Current interest in these materials triggered further research on a practical level, as in for exam-

SSDI 0167-6636(94)00074-3

ple Otsuka and Shimizu (1986), but also on a fundamental level, as in the work of for instance Patoor et al. (1987) and Fisher et al. (1994). The phase transformation in SMA is essentially reversible. Usually, temperature is the driving force for reverse transformation, but it is also possible to induce reverse transformation by stress (Sun and Hwang, 1993b). If, for instance, the material behavior is pseudoelastic, reversible transformation occurs directly upon unloading. Another characteristic of the phase transformations in SMA is that they generally involve only shear transformation strains. In fact, in this study, we shall use the term SMA generically for materials that exhibit pure shear transformation behavior.

The tetragonal to monoclinic phase transformation in zirconia containing ceramics is well-known to give rise to a substantial toughening effect (see Evans and Heuer, 1980). Although this transformation was immediately recognized as being martensitic, it was not until a few years ago that both shear and dilatation transformation strains were measured in partially stabilized zirconia (PSZ) by Chen and Reyes-Morel (1986, 1987) and that pseudoelasticity and shape memory effects were determined experimentally in tetragonal zirconia polycrystal (TZP) by Reyes-Morel et al. (1988). Since these investigations, the nonlinear deformation behavior of these materials is often referred to as transformation plasticity. Sun et al. (1991) proposed a constitutive model to describe these phenomena, taking into account both dilatation and shear effects of the transformation. This model has recently been adopted by Stam et al. (1994) to study the influence of the tetragonal to monoclinic transformation on the crack growth resistance in these materials. Full field finite element analyses have confirmed that transformation-induced shear strains substantially enhance the R-curve behavior, as compared to when the transformation is assumed to be purely dilatant (Budiansky et al. 1983). Thus, both experimental work and theoretical modelling have now provided clear evidence that, even though twinning occurs, net shear transformation strains contribute to the toughness of these materials.

This and other analyses of transformation-induced toughening in zirconia containing ceramics (e.g. Budiansky et al. 1983; Hom and McMeeking, 1990) so far have assumed that the phase transformation is completely irreversible. However, there is some experimental evidence that reversible transformation does occur in the work by Marshall and James (1986) and in the dynamic compression tests by Subhash and Nemat-Nasser (1993). However in the latter work, substantial strain-rate effects have been observed as well as significant microcracking, which will both have an influence on the overall behavior, so that care must be exercised in relating these experimental results to the considerations in the present paper.

The purpose of the present paper is to explore the sole influence of reversibility of phase transformations on crack growth resistance under quasi-static conditions. We shall do so by adopting the constitutive theory of Sun et al. (1991) which is applicable to zirconia-containing ceramics, as mentioned above, as well as to SMA, as discussed by Sun and Hwang (1993a,b). The constitutive model will be briefly reviewed in Section 2. Crack growth under mode I loading conditions will be studied numerically, assuming small-scale transformation conditions (see Section 3). The main arguments will be carried in coordinate-free tensor notation, where tensors are denoted by boldface italic characters irrespective of their rank (which will be clear from the context). The tensor product is denoted with $\otimes$ and a dot denotes the inner or scalar product between two tensors. The following operators apply ($\boldsymbol{A} = A_{ij}\boldsymbol{e}_i \otimes \boldsymbol{e}_j$, $\boldsymbol{B} = B_{ij}\boldsymbol{e}_i \otimes \boldsymbol{e}_j$, $\boldsymbol{L} = L_{ijkl}\boldsymbol{e}_i \otimes \boldsymbol{e}_j \otimes \boldsymbol{e}_k \otimes \boldsymbol{e}_l$; $\boldsymbol{e}_i$ is a Cartesian basis): $\boldsymbol{A} \cdot \boldsymbol{B} = A_{ij}B_{ij}$, $\boldsymbol{LA} = L_{ijkl}A_{kl}\boldsymbol{e}_i \otimes \boldsymbol{e}_j$, $\mathrm{tr}\,\boldsymbol{A} = A_{kk}$. The second-order unit tensor is $\boldsymbol{I}$. A superposed dot denotes the time derivative or rate.

2. Material model

2.1. Constitutive equations

The complexity of the transformation problem is reduced by assuming that a material sample can be identified which is small compared to all macroscopic dimensions, but which is large

enough that statistical averaging over all transformable particles is meaningful. Such a material sample can then be treated as a continuum element for which all (macroscopic) quantities are averages over the sample. Phenomena on a smaller scale are discarded. This means, for instance, that local stress and strain fields around individual particles are not considered, but only the macroscopic average of these fields over all particles in the sample.

When deriving, within such an approach, the transformation plasticity model, Sun et al. (1991) assumed the continuum element to consist of a large number of transformable inclusions (referred to with index I) which are embedded coherently in an elastic matrix (referred to with index M). Microscopic quantities (on a lower scale then for which the continuum element is derived) will be referred to with lower case characters. The macroscopic quantities denoted with uppercase symbols are found by taking the volume average $\langle\ \rangle$ of the microscopic quantities denoted by lower case characters over the element. For instance, the microscopic stress and strain tensors are indicated by $\boldsymbol{\sigma}$ and $\boldsymbol{\varepsilon}$, respectively, and with a given volume fraction of second phase (transformable metastable tetragonal inclusions) f^{m}, the relation between microscopic and macroscopic stresses $\boldsymbol{\Sigma}$ is

$$\boldsymbol{\Sigma} = \langle \boldsymbol{\sigma} \rangle_V = \frac{1}{V}\int_V \boldsymbol{\sigma}\, \mathrm{d}V = f\langle \boldsymbol{\sigma} \rangle_{V_\mathrm{I}} + (1-f)\langle \boldsymbol{\sigma} \rangle_{V_\mathrm{M}}. \tag{1}$$

Here the volume of the element, matrix and inclusions is given by V, V_M and V_I, respectively, and f is the actual fraction of transformed material which is obviously smaller than or equal to f^{m}. The macroscopic strains $\boldsymbol{E}$ are assumed to be small, and assuming isothermal deformations, they can be decomposed into an elastic part $\boldsymbol{E}^{\mathrm{e}}$ and a "plastic" part $\boldsymbol{E}^{\mathrm{p}}$ due to the p → m transformation in the inclusions,

$$\boldsymbol{E} = \boldsymbol{E}^{\mathrm{e}} + \boldsymbol{E}^{\mathrm{p}} = \boldsymbol{M}^0 \boldsymbol{\Sigma} + f\langle \boldsymbol{\varepsilon}^{\mathrm{p}} \rangle_{V_\mathrm{I}}. \tag{2}$$

Here $\boldsymbol{M}^0 = (\boldsymbol{L}^0)^{-1}$, with $\boldsymbol{L}^0$ being the elastic moduli of both inclusions and matrix. The p → m phase transition may involve dilatation as well as shear strains within the inclusion, thus suggesting a split in the plastic strain into a dilatant part and a deviatoric part, designated with superscripts d and s, respectively,

$$\boldsymbol{E}^{\mathrm{p}} = \boldsymbol{E}^{\mathrm{pd}} + \boldsymbol{E}^{\mathrm{ps}} = f\langle \boldsymbol{\varepsilon}^{\mathrm{pd}} \rangle_{V_\mathrm{I}} + f\langle \boldsymbol{\varepsilon}^{\mathrm{ps}} \rangle_{V_\mathrm{I}}. \tag{3}$$

The rates of plastic strain during progressive transformation, $\dot{f} > 0$, can be obtained by the straightforward differentiation of (3); but they can also be obtained from the average of the transformation strain $\boldsymbol{\varepsilon}^{\mathrm{p}}$ over the freshly transformed inclusions (per unit time) occupying volume $\mathrm{d}V_\mathrm{I}$, i.e.

$$\begin{aligned}\dot{\boldsymbol{E}}^{\mathrm{p}} &= \dot{\boldsymbol{E}}^{\mathrm{pd}} + \dot{\boldsymbol{E}}^{\mathrm{ps}} \\ &= \dot{f}\langle \boldsymbol{\varepsilon}^{\mathrm{pd}} \rangle_{V_\mathrm{I}} + \dot{f}\langle \boldsymbol{\varepsilon}^{\mathrm{ps}} \rangle_{V_\mathrm{I}} \\ &\quad + f\overline{\langle \boldsymbol{\varepsilon}^{\mathrm{pd}} \rangle_V^{\mathrm{I}}} + f\overline{\langle \boldsymbol{\varepsilon}^{\mathrm{ps}} \rangle_V^{\mathrm{I}}} \\ &= \dot{f}\langle \boldsymbol{\varepsilon}^{\mathrm{pd}} \rangle_{\mathrm{d}V_\mathrm{I}} + \dot{f}\langle \boldsymbol{\varepsilon}^{\mathrm{ps}} \rangle_{\mathrm{d}V_\mathrm{I}}.\end{aligned} \tag{4}$$

The dilatant part $\boldsymbol{\varepsilon}^{\mathrm{pd}}$ within each inclusion can be given in terms of the constant stress-free lattice volume dilatation $\varepsilon^{\mathrm{pd}}$,

$$\langle \boldsymbol{\varepsilon}^{\mathrm{pd}} \rangle_{\mathrm{d}V_\mathrm{I}} = \langle \boldsymbol{\varepsilon}^{\mathrm{pd}} \rangle_{V_\mathrm{I}} \equiv \boldsymbol{\varepsilon}^{\mathrm{pd}} = \varepsilon^{\mathrm{pd}} \boldsymbol{I}. \tag{5}$$

The average deviatoric part $\boldsymbol{E}^{\mathrm{ps}}$ is significantly less than the stress-free lattice shear strain because of twinning (see Zhang and Lam, 1994). Based on earlier work of Reyes-Morel and Chen (1988) and Reyes-Morel et al. (1988), this part is specified through its rate of change $\dot{f}\langle \boldsymbol{\varepsilon}^{\mathrm{ps}} \rangle_{\mathrm{d}V_\mathrm{I}}$, which is assumed to depend on the average stress $\boldsymbol{\sigma}^{\mathrm{M}} = \langle \boldsymbol{\sigma} \rangle_{V_\mathrm{M}}$ in the matrix according to

$$\langle \boldsymbol{\varepsilon}^{\mathrm{ps}} \rangle_{\mathrm{d}V_\mathrm{I}} = A \frac{\boldsymbol{s}^{\mathrm{M}}}{\sigma_{\mathrm{e}}^{\mathrm{M}}}, \quad \sigma_{\mathrm{e}}^{\mathrm{M}} = \sqrt{\tfrac{3}{2} tr\left(\boldsymbol{s}^{\mathrm{M}}\right)^2}, \tag{6}$$

with A a material function, which can be considered as a measure of the constraint of the elastic matrix. Here $\boldsymbol{s}^{\mathrm{M}}$ is the matrix stress deviator, defined by $\boldsymbol{s}^{\mathrm{M}} = \boldsymbol{\sigma}^{\mathrm{M}} - \sigma_{\mathrm{m}}^{\mathrm{M}} \boldsymbol{I}$ with $\sigma_{\mathrm{m}}^{\mathrm{M}} = \frac{1}{3}\mathrm{tr}\ \boldsymbol{\sigma}^{\mathrm{M}}$ being the matrix mean stress, and $\sigma_{\mathrm{e}}^{\mathrm{M}}$ is the von Mises stress in the matrix, which will be specified later. When $\sigma_{\mathrm{e}}^{\mathrm{M}} = 0$, A should be put zero because there is no stress bias. However, experimental data of Chen and Reyes-Morel (1986, 1987) and Reyes-Morel and Chen (1988) show that under proportional loading the value of A is

almost constant during the whole transformation process. Sun et al. (1991) have emphasized that (6) is a macroscopic constitutive relationship that is assumed to apply to the ensemble of transformable particles mentioned in the beginning of the section. The deviatoric transformation strain over individual transformed particles will not depend on the local matrix stresses in such a simple manner. Firstly, twinning in a particle will occur in well-defined directions on specific crystallographic planes. Furthermore, the amount of twinning within particles is dependent on the particle size (see, e.g. Evans and Cannon, 1986). Although much research has been devoted to nucleation and twinning in a single particle, these are still phenomena which are not well understood and need further attention. However, since in this model many grains with different orientations are considered within d V_I, Sun et al. (1991) argue that (6) is an acceptable approximation in the average sense. Combining the expressions (4)–(6), the plastic strain-rate is found as

$$\dot{\boldsymbol{E}}^{\mathrm{p}} = \dot{f}\left(\varepsilon^{\mathrm{pd}}\boldsymbol{I} + \langle \boldsymbol{\varepsilon}^{\mathrm{ps}} \rangle_{\mathrm{d}\, V_I}\right). \tag{7}$$

Adopting Eshelby's (1961) solution for a spherical inclusion in an infinite extended elastic body and the averaging method of Mori and Tanaka (1973), the deviatoric and mean matrix stresses, $\boldsymbol{s}^{\mathrm{M}}$ and $\sigma_{\mathrm{m}}^{\mathrm{M}}$, respectively, are found to be related to the macroscopic stress $\boldsymbol{\Sigma}$ by

$$\boldsymbol{s}^{\mathrm{M}} = \boldsymbol{S} - fB_1\langle \boldsymbol{\varepsilon}^{\mathrm{ps}} \rangle_{V_I}, \quad \sigma_{\mathrm{m}}^{\mathrm{M}} = \Sigma_{\mathrm{m}} - fB_2\varepsilon^{\mathrm{pd}}. \tag{8}$$

Here, $\boldsymbol{S} = \boldsymbol{\Sigma} - \Sigma_{\mathrm{m}}\boldsymbol{I}$ and $\Sigma_{\mathrm{m}} = \frac{1}{3}\,\mathrm{tr}\,\boldsymbol{\Sigma}$ are the deviatoric and mean components of the macroscopic stress $\boldsymbol{\Sigma}$, and

$$B_1 = 2G\frac{5\nu - 7}{15(1-\nu)}, \quad B_2 = 2B\frac{2\nu - 1}{1-\nu}, \tag{9}$$

with G the shear modulus, B the bulk modulus and ν Poisson's ratio of the matrix as well as the inclusion, all being related in the standard way to Young's modulus E,

$$G = \frac{E}{2(1+\nu)}, \quad B = \frac{E}{3(1-2\nu)}. \tag{10}$$

The constitutive theory must be completed with transformation conditions and an evolution relation in terms of $\dot{f}$. Sun et al. (1991) give the following conditions for forward or reverse transformations to occur:

Forward:

$$F_+\left(\boldsymbol{\Sigma}, f, T, \langle \varepsilon^{\mathrm{ps}} \rangle_{V_I}\right) = \tfrac{2}{3}A\sigma_{\mathrm{e}}^{\mathrm{M}} + 3\sigma_{\mathrm{m}}^{\mathrm{M}}\varepsilon^{\mathrm{pd}} - C_0(T, f) = 0; \tag{11}$$

Reverse:

$$F_-\left(\boldsymbol{\Sigma}, f, T, \langle \boldsymbol{\varepsilon}^{\mathrm{ps}} \rangle_{V_I}\right) = \tfrac{2}{3}A\sigma_{\mathrm{e}}^{\mathrm{M}} + 3\sigma_{\mathrm{m}}^{\mathrm{M}}\varepsilon^{\mathrm{pd}} - \tilde{C}_0(T, f) = 0. \tag{12}$$

The function $C_0(T, f)$ for forward transformation depends on the dissipation D_0 (due to, e.g. interface friction), on the difference in surface energy A_0, on the free chemical energy difference $\Delta G_{\mathrm{p}\to\mathrm{m}}(T)$ associated with the transformation (which depends on the temperature T), and on the elastic energy associated with the interaction between transformed particles and matrix,

$$C_0(T, f) = D_0 + A_0 + \Delta G_{\mathrm{p}\to\mathrm{m}}(T) - \tfrac{1}{3}B_1A^2 - \tfrac{3}{2}B_2\left(\varepsilon^{\mathrm{pd}}\right)^2 + \alpha B_0 f. \tag{13}$$

The last term in (13) is introduced to incorporate the common experimental observation that the resistance to transformation tends to increase with increasing volume fraction of transformed material; here, this "hardening" is governed by the parameter α. Note that this hardening term is due to processes on microstructural scale, such as

(i) particle size dependence: it takes a higher stress level to transform smaller particles;

(ii) crystallographic orientation: favorably oriented planes transform first, and

(iii) the mutual interference of transformed regions: transformation of a particle will cause a relaxation of the stresses in its surrounding.

Subhash and Nemat-Nasser (1993) give a detailed discussion of these microstructural aspects, based on their dynamic loading experiments on TZP and PSZ materials. As the constitutive model is derived for the macroscopic scale, considering many transformable particles in one constitutive element, the hardening effect did not follow from the derivation itself and Sun et al. (1991) introduced the last term in (13) on mere phenomeno-

logical grounds. The parameter B_0 in (13) is a bulk modulus-like parameter defined by

$$B_0 = \frac{4G(1+\nu)(\varepsilon^{pd})^2}{1-\nu} + \frac{GA^2(28-20\nu)}{45(1-\nu)}, \quad (14)$$

The corresponding function $\tilde{C}(T, f)$ in the reverse transformation condition (12) is given in similar way by

$$\begin{aligned}\tilde{C}_0(T, f) &= -D_0 + A_0 + \Delta G_{p\to m}(T) \\ &\quad - \tfrac{1}{3}B_1A^2 - \tfrac{3}{2}B_2\varepsilon^{pd^2} + \alpha B_0 f \\ &= C_0(T, f) - 2D_0, \end{aligned} \quad (15)$$

thus emphasizing that the reversibility of the transformation is controlled by the dissipation associated with the phase transformation.

The growth rate of the fraction transformed tetragonal phase, $\dot{f}$, follows from the consistency condition $\dot{F}_+ = 0$ or $\dot{F}_- = 0$, and is found for either one of the transformation directions to be given by

$$\dot{f} = \frac{\langle \boldsymbol{\varepsilon}^{ps} \rangle_{dV_1} \cdot \dot{\boldsymbol{S}} + 3\varepsilon^{pd}\dot{\Sigma}_m}{\frac{2}{3}B_1A^2 + 3B_2(\varepsilon^{pd})^2 + \alpha B_0}. \quad (16)$$

Expression (16) holds as long as the transformation progresses, i.e.

- when the current stress state satisfies the forward transformation condition (11) while there is still a transformable fraction left, $f < f^m$, and the transforming fraction $\dot{f}$ is positive ($p \to m$), or
- the current stress state satisfies the reverse transformation condition (12) while there is still a transformable fraction left, $f > 0$, and the transforming fraction $\dot{f}$ is negative ($p \leftarrow m$).

Finally, the constitutive equations will be rearranged into a form which is necessary for the subsequent numerical analysis. With the relation (2) between strain rates and stress rates, and introducing the following definitions,

$$\boldsymbol{T} \equiv \varepsilon^{pd}\boldsymbol{I} + A\frac{\boldsymbol{s}^M}{\sigma_c^M}, \quad \text{and}$$

$$g \equiv \tfrac{2}{3}B_1A^2 + 3B_2(\varepsilon^{pd})^2 + \alpha B_0(\varepsilon^{pd})^2, \quad (17)$$

one can derive the following rate constitutive equations

$$\dot{\boldsymbol{\Sigma}} = \boldsymbol{L}\dot{\boldsymbol{E}}, \quad (18)$$

where the tensor of instantaneous moduli $\boldsymbol{L}$ is defined by

$$\boldsymbol{L} = \begin{cases} \boldsymbol{L}^0 - \dfrac{1}{g}\dfrac{\boldsymbol{L}^0\boldsymbol{T}\otimes\boldsymbol{T}\boldsymbol{L}^0}{1+\dfrac{1}{g}(\boldsymbol{T}\cdot\boldsymbol{L}^0\boldsymbol{T})}, \\ \quad \text{when} \begin{cases} F_+ = 0 \text{ and } \dot{f} > 0, \text{ or} \\ F_- = 0 \text{ and } \dot{f} < 0; \end{cases} \\ \boldsymbol{L}^0, \quad \text{when} \begin{cases} F_+ \neq 0 \text{ or } \dot{f} < 0, \text{ or} \\ F_- \neq 0 \text{ or } \dot{f} > 0. \end{cases} \end{cases} \quad (19)$$

Details may be found in Stam (1994). On the transformation branch, the stiffness tensor $\boldsymbol{L}$ is comprised of the linear elastic stiffness tensor $\boldsymbol{L}^0$ and a nonlinear part due to the transformation which is similar to the well-known plastic moduli in elastoplasticity. It is of considerable importance to note that the moduli $\boldsymbol{L}$ possess the following symmetry when expressed in their Cartesian components L_{ijkl}:

$$L_{ijkl} = L_{klij}, \quad (20)$$

in addition to the obvious symmetries in ij and kl.

2.2. Material parameters

With a view on the application to different materials, three types of transformation behavior are distinguished, viz.:

(*i*) purely dilatant transformation behavior: the shear component of the transformation is completely relaxed by twinning ($A = 0$),

(*ii*) dilatant and shear transformation behavior, and

(*iii*) purely shear transformation behavior: the volume of the parent phase and the martensitic phase is identical ($\varepsilon^{pd} = 0$).

The latter of these types is applicable to SMA materials (cf. Sun and Hwang, 1993a,b); the second type applies to ceramics containing zirconia, while the first is a limiting case of the second,

which is discussed here mainly for comparison with earlier studies of Budiansky et al. (1983) and Hom and McMeeking (1990). Dimensional analysis and close examination of the governing constitutive equations reveal that the material model is completely characterized by the following non-dimensional groups:

purely dilatant:

$$\nu,\ \omega \equiv \frac{9Ef^{m}(\varepsilon^{pd})^{2}}{C(T,0)}\left[\frac{1+\nu}{1-\nu}\right],$$

$$\alpha,\ M \equiv \tilde{C}_0(T,0)/C_0(T,0), \tag{21a}$$

dilatant and shear:

$$\nu,\ \omega \equiv \frac{9Ef^{m}(\varepsilon^{pd})^{2}}{C(T,0)}\left[\frac{1+\nu}{1-\nu}\right],$$

$$\alpha,\ M \equiv \tilde{C}_0(T,0)/C_0(T,0),\ A, \tag{21b}$$

purely shear:

$$\nu,\ \omega' \equiv \frac{4Ef^{m}A^{2}}{9C(T,0)}\left[\frac{1+\nu}{1-\nu}\right],$$

$$\alpha,\ M \equiv \tilde{C}_0(T,0)/C_0(T,0). \tag{21c}$$

The parameter ω in (21a,b) governs the strength of the transformation and was originally defined by Amazigo and Budiansky (1988) for purely dilatant transformation behavior. However, when also transformation shear components develop during transformation, the transformation can still be characterized by ω, but along with the amount of macroscopic shear transformation strain being governed by material parameter A. When the dilatant component of the transformation strain vanishes, ω has to be redefined. Using the same concept of "strength of the transformation", we here define ω' by replacing the dilatant transformation strain $3\varepsilon^{pd}$ in the definition of ω by the equivalent transformation strain ε_e^p. With the usual definition of the equivalent strain $\varepsilon_e^p \equiv \sqrt{\frac{2}{3}\,\mathrm{tr}(\boldsymbol{\varepsilon}^{ps})^2}$ we find that $\varepsilon_e^p = \frac{2}{3}A$, which is used in the definition of ω'. It must be noted that in the latter case, the material parameter A is no longer an independent material parameter.

Finally, the reversible transformation condition has to be defined. Therefore we have introduced in (21) the parameter M, which defines the relative position of the reverse transformation condition (11) to forward transformation condition (12). For four values of M the macroscopic uniaxial stress–strain relations (Σ_{11} versus E_{11}) are plotted in Fig. 1 to show the meaning of the parameter M. The curves are obtained using the

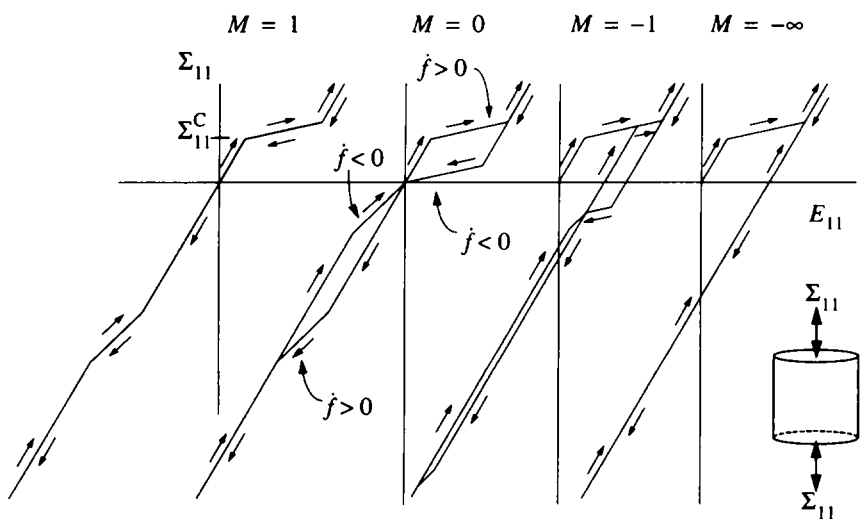

Fig. 1. Stress–strain relations for a uniaxial tension–compression–tension loading program for $h_0 = 1.0$, $\alpha = 1.25$ and $M = [1, 0, -1, -\infty]$.

constitutive equations discussed in the previous section, and incrementally prescribing the stress in axial direction x_1, so that the specimen passes through a cycle of tension, compression and tension. For experimental work on this matter, see Bowman et al. (1987). In all cases, the material behavior is similar during the first tensile loading stage. The material behaves linear elastically up to a certain critical transformation stress $\Sigma^C = C_0(T, 0)/(\frac{2}{3}A + \varepsilon^{pd})$, according to (11), when the material starts to transform, up to the point where the material is fully transformed, $f = f^m$. After that, the response is linear elastic again. Note that during transformation, the incremental response is linear because of the linear dependence of C_0 in (13) on f. When the specimen is unloaded, the differences in response as a result from the different choices of M arise.

As shown in Fig. 1, for $M = 1$ the material will immediately show a reverse transformation response upon unloading when the stress level is reached where the forward transformation was completed. Obviously, reverse transformation is completed when all material is converted to the original crystal structure ($f = 0$) and the stress is equal to the critical (forward) transformation stress $\Sigma_{11} = \Sigma^C$. Then the material response is linear elastic again. The material behavior is linear elastic up to the point where the critical forward transformation stress in the compression regime is reached. Forward transformation occurs up to completion $f = f^m$, followed by linear elastic behavior, similar to the behavior under tension.

For $M = 0$, no direct reverse transformation upon unloading occurs, but all transformation strains are zero when the material is stress-free. This is true for the tensile regime as well as for the compression regime.

For $M = -1$, reverse transformation does not occur until the specimen reaches a certain stress level in the compression regime. Theoretically, the reverse transformation is completed when $f = 0$ and $\Sigma_{11} = -\Sigma^C$, but in uniaxial tension it turns out to be impossible to convert all the transformation strain. Before all material has been transformed back, the transformation criterion is no longer met and the material becomes linear elastic again. Linear elasticity is maintained until the stress level for forward transformation in the compression regime is met. There the remaining transformable phase is transformed up to $f = f^m$. Upon unloading the transformed phase is partially transformed back again, before the behavior becomes linear elastic. It may be clear that in this experiment, part of the transformation strain is permanent while the other part is reversible. This effect is caused by the volume change of the transformation, which does not occur for SMA materials. For $M = -\infty$, no reverse transformation occurs, but even for higher values of M reverse transformation may be impossible.

At this point, it seems pertinent to make note of the notions of subcritical and supercritical transformations, as introduced by Budiansky et al. (1983) for purely dilatant transformations ($A = 0$). Such transformations are called supercritical when they occur spontaneously and immediately to completion. This is possible when the incremental governing equations cease to be elliptic, so that discontinuities in the stress and strain fields are possible. In the case of subcritical transformations, the governing equations remain elliptic and the material can exist in stable partially transformed states. Stam et al. (1994) have recently generalized these notions in terms of a localization condition. For typical values of the material parameters listed in (21a,b), it was found that dilatant and shear transformations remain subcritical as long as the hardening parameter α satisfies the condition $\alpha \geq 1$. In this paper, we wish to confine our attention to subcritical transformations and we therefore limit ourselves to values $\alpha \geq 1$.

3. Problem formulation and method of solution

The problem studied here to gain insight in the effect of reverse transformations is similar to that used in Stam et al. (1994); we shall give a brief exposition for completeness, and for further details refer to Stam et al. (1994).

We study the growth of straight crack under mode I loading conditions by assuming that the

zone in which the material undergoes the phase transformation discussed above, is very small compared to the crack length a (see Fig. 2). For the resulting small-scale transformation problem we can confine our attention to a (circular) region around the crack tip with the boundary conditions along the circumference according to the well-known linear elastic field characterized by the stress intensity factor K^{APP} corresponding to the applied mode I loading. Moving from this boundary inwards to the crack tip, we will first encounter a region close to the tip where the material is partially transformed, i.e. $f < f^m$, and even closer to the crack tip, we expect to find a region where the material is completely transformed, i.e. $f = f^m$. As discussed before, the incremental response of the material inside the latter, fully transformed zone is also linear elastic, and the fields in that zone right near the crack tip are characterized by an unknown stress intensity factor K^{TIP}.

Prior to any transformation, $K^{APP} = K^{TIP}$ obviously, but once transformation starts under monotonically increasing K^{APP}, we will have $K^{APP} \neq K^{TIP}$ in general ($K^{APP} = K^{TIP}$ prior to crack growth only if the transformation involves a dilatation (Budiansky et al., 1983 or Stam et al., 1994)). Crack propagation is taken to occur when K^{TIP} attains the critical value K^C, i.e. the fracture toughness of the material at the crack front. Upon crack advance, transformed material will appear in the wake of the crack, and the tip is shielded as a result of the transformation strains. Thus, in order to maintain crack growth, K^{APP} must be continually adapted with increasing crack advance Δa (R-curve behavior). A convenient measure for the increase of the effective crack growth resistance of the material is the ratio

$$K^{APP}/K^{TIP} = K^{APP}/K^C = 1 - \Delta K^{TIP}/K^C, \tag{22}$$

with ΔK^{TIP} being defined by

$$\Delta K^{TIP} \equiv K^{TIP} - K^{APP}.$$

Note that $\Delta K^{TIP} < 0$ when toughening takes place.

The value of the near-tip intensity reduction ΔK^{TIP} to be substituted into (22) is evaluated by an extension of a domain integral technique suggested by Budiansky et al. (1983),

$$\Delta K^{TIP} = \int_\Omega \mathrm{d}K^{TIP}\, \mathrm{d}A, \tag{23}$$

where Ω represents the transformed region. In this approach, use is made of exact relationships derived by Hutchinson (1974) to calculate the intensity enhancement $\mathrm{d}K^{TIP}$ in an elastic medium caused by in-plane stress-free transformation strains $E^p_{\alpha\beta}$ in an infinitesimal area at any point within the transformation zone.

$$\mathrm{d}K^{TIP} = \frac{1}{\sqrt{8\pi}} \frac{E}{(1-\nu^2)} r^{-3/2} M(E^p_{\alpha\beta}, \beta), \tag{24}$$

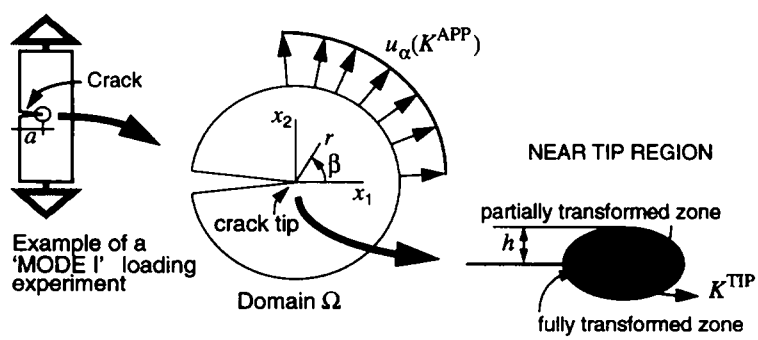

Fig. 2. The small-scale transformation assumption and the corresponding boundary value problem for a semi-infinite crack subjected to mode I loading.

where

$$M(E^{p}_{\alpha\beta}, \beta) = (E^{p}_{11} + E^{p}_{22}) \cos\tfrac{3}{2}\beta + 3E^{p}_{12} \cos\tfrac{5}{2}\beta \sin\beta + \tfrac{3}{2}(E^{p}_{22} - E^{p}_{11}) \sin\beta \sin\tfrac{5}{2}\beta \quad (25)$$

given by Lambropoulos (1986). The plane strain, stress-free transformation strains $E^{p}_{\alpha\beta}$ to be substituted for the present constitutive model, are given by

$$E^{p}_{11} = (1+\nu) f \varepsilon^{pd} + f\left[\langle \varepsilon^{ps}_{11}\rangle_{V_1} - \nu\left(\langle \varepsilon^{ps}_{11}\rangle_{V_1} + \langle \varepsilon^{ps}_{22}\rangle_{V_1}\right)\right],$$

$$E^{p}_{22} = (1+\nu) f \varepsilon^{pd} + f\left[\langle \varepsilon^{ps}_{22}\rangle_{V_1} - \nu\left(\langle \varepsilon^{ps}_{11}\rangle_{V_1} + \langle \varepsilon^{ps}_{22}\rangle_{V_1}\right)\right],$$

$$E^{p}_{12} = f\langle \varepsilon^{ps}_{12}\rangle_{V_1}. \quad (26)$$

The problem is solved numerically in a linear incremental fashion and with a standard finite element discretization of the boundary value problem. Quadrilateral elements are used, each of which is built up of four constant strain elements. The mesh that has been used is shown in Fig. 3. The formulation of the numerical procedure relies on the similarity of the constitutive relations discussed in Section 2.1, with those in the usual time-independent elastoplasticity models with an associative flow rule. At each increment i, the nodal displacement increments $\Delta \boldsymbol{u}^{(i)}$ are solved from

$$\boldsymbol{K}^{(i)} \Delta \boldsymbol{u}^{(i)} = \Delta \boldsymbol{F}^{(i)} - (\boldsymbol{D}^{T} \boldsymbol{\Sigma}^{(i)} - \boldsymbol{F}^{(i)}),$$

$$\text{with } \boldsymbol{K}^{(i)} = \boldsymbol{D}^{T} \boldsymbol{S}^{(i)} \boldsymbol{D}, \quad (27)$$

where $\Delta \boldsymbol{F}^{(i)}$ is the vector of nodal load increments and where the stiffness matrix $\boldsymbol{S}^{(i)}$ is determined by the instantaneous moduli $\boldsymbol{L}$ appearing in (19). The bracket term in the right-hand side of (27) is an equilibrium correction based on the current discrete stress state, collected formally in the vector $\boldsymbol{\Sigma}^{(i)}$. With these $\Delta \boldsymbol{u}^{(i)}$, the state in each integration point is updated in the usual manner for geometrically linear elastoplasticity problems. If the critical stress level is reached so that the transformation criterion $F_{+} = 0$ is satisfied, the incremental volume fraction of transformed material $\Delta f^{(i)}$ is obtained from the incremental version of (16), and similarly for the reverse transformation criterion $F_{-} = 0$. The incremental change of $\boldsymbol{E}^{ps}$ at each integration point is determined from (4), and the updated value $\langle \boldsymbol{\varepsilon}^{ps}\rangle_{V_1}^{(i+1)}$ according to (6) is used in (26) for the computation of the updated value $\Delta K^{TIP}_{(i+1)}$. If the resulting value $K^{TIP}_{(i+1)} = K^{C}$, crack advance is simulated by a nodal release technique. Details of the numerical procedure may be found in Stam et al. (1994) and Stam (1994).

The stress intensity change at the crack tip due to the transforming spots, ΔK^{TIP}, is computed numerically by a 13-point Gaussian integration within each element. Near the crack tip (within a radius of 3 elements) the integration is carried out analytically to take care of the singularity in (24) at the tip. The toughness increase will be expressed in $K^{APP}(\Delta a)/K^{C}$, while all length scales will be normalized by the length scale L defined by Stam et al. (1994),

$$L = \frac{2}{9\pi}\left[\frac{K^{C}\{A(1-2\nu) + 3\varepsilon^{pd}(1+\nu)\}}{C(T,0)}\right]^{2}. \quad (28)$$

4. Results

Throughout the analysis we take $\nu = 0.3$, but various combinations of the other material parameters ω/ω', α, A, and in particular M are considered to study their effect of reverse transformation on toughness development and on the size and shape of the transformation zone. We show results of crack growth computations for all three types of transformation behavior. Listed in (21a) for the purely dilatant transformation behavior ($A = 0$), we have performed a large number of computations with $\omega = 5$ to study the influence of the reverse transformation. Here, only the results for $\omega = 5$, $\alpha = 1.00$ and $M = [-1, 0, 0.50, 0.75, 1]$ are shown. For an overview of the results presented here we refer to Fig. 4; more results can be found in Stam and Van der Giessen (1993) or Stam (1994).

For the dilatant and shear transformation behavior we proceed from the earlier parameter

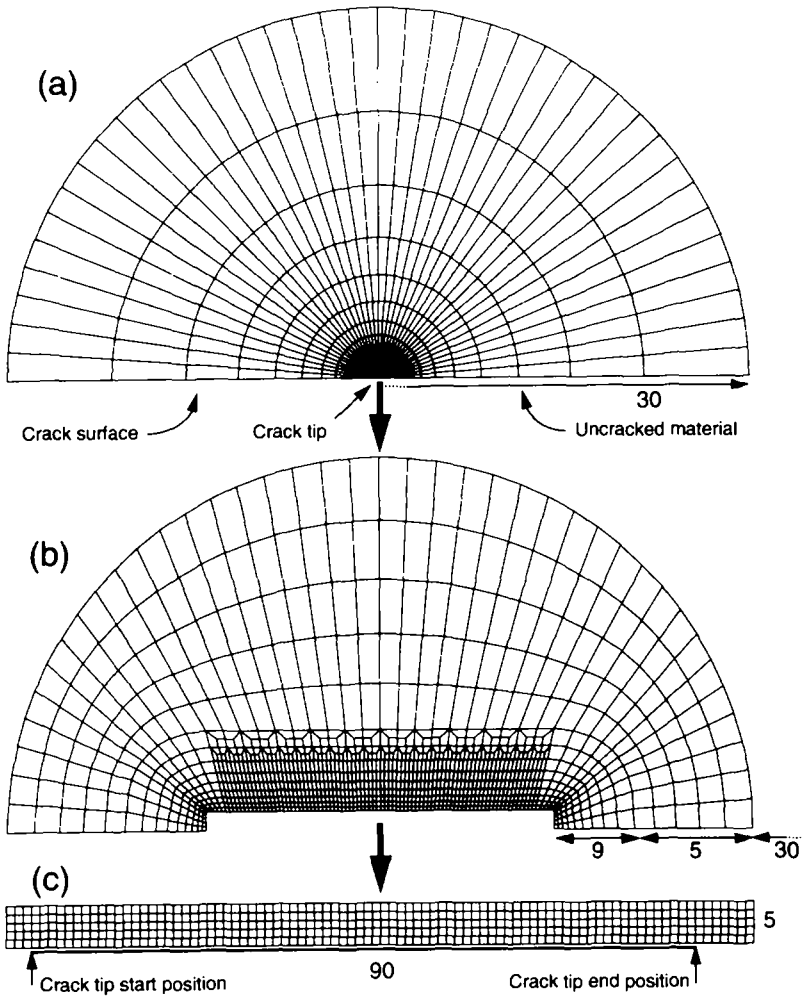

Fig. 3. The finite element mesh used to analyze the small-scale crack growth problem. The mesh comprises 2770 quadrilateral elements and 2880 nodes. Crack growth by nodal release is permitted to occur over a span of 80 nodes.

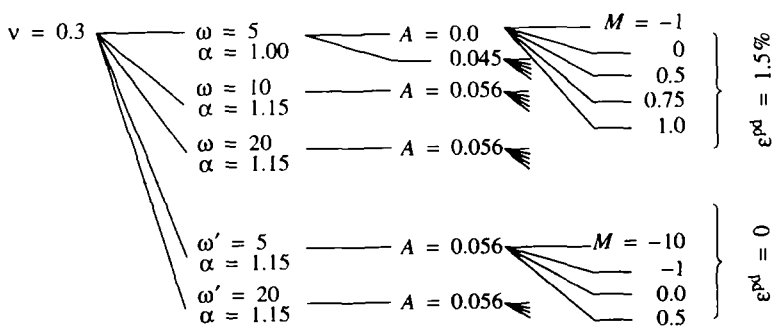

Fig. 4. The composition of the parameter study.

studies for $\omega = 5$ and 10 (Stam et al., 1994) and for $\omega = 15$ and 20 (Stam and Van der Giessen, 1994) for irreversible transformation. For each value of ω, the hardening parameter α is chosen to be either 1 or 1.15. The smallest value of α is chosen to be 1 to avoid localization, so that the transformation remains subcritical, over a wide range of material parameters (see Section 2.2). The studies with material parameters $\omega = 10$ and 20 more or less cover the experimental values of the material parameters given by Sun et al. (1991) for various materials, which vary from $\omega = 11$ for

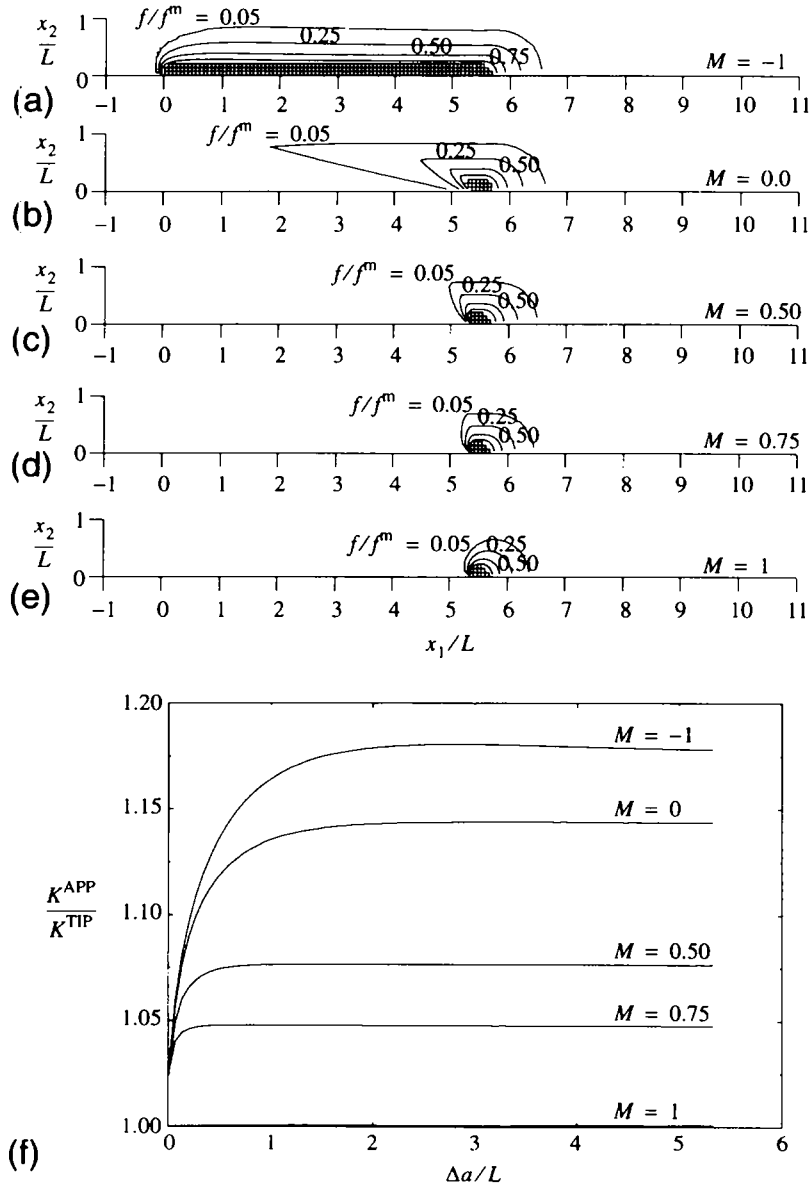

Fig. 5. Transformation zones (a–e) when $\Delta a = 5.33L$, and the crack growth resistance curve (f) for $\omega = 5$, $\alpha = 1.25$, $A = 0.0$ (purely dilatant transformations) and $M = -1$ to 1.

a typical PSZ to $\omega = 24$ for a typical TZP material. In these computations the macroscopic transformation shear parameter A is taken to be 0.056 (and $A = 0.045$ for $\omega = 5$) which is in the experimental range (this corresponds to values of $h_0 = A/3\varepsilon^{pd}$ equals 1.25 (and 1.00), which were used in Stam et al. (1994)). The value $\alpha = 1.15$ has been chosen as a representative value for the experimental values of $\alpha = 1.16$ and 1.2 for TZP and PSZ, respectively, given by Sun et al. (1991).

Finally, results for SMA, with no dilatant component of the transformation strain ($\varepsilon^{pd} = 0$) are

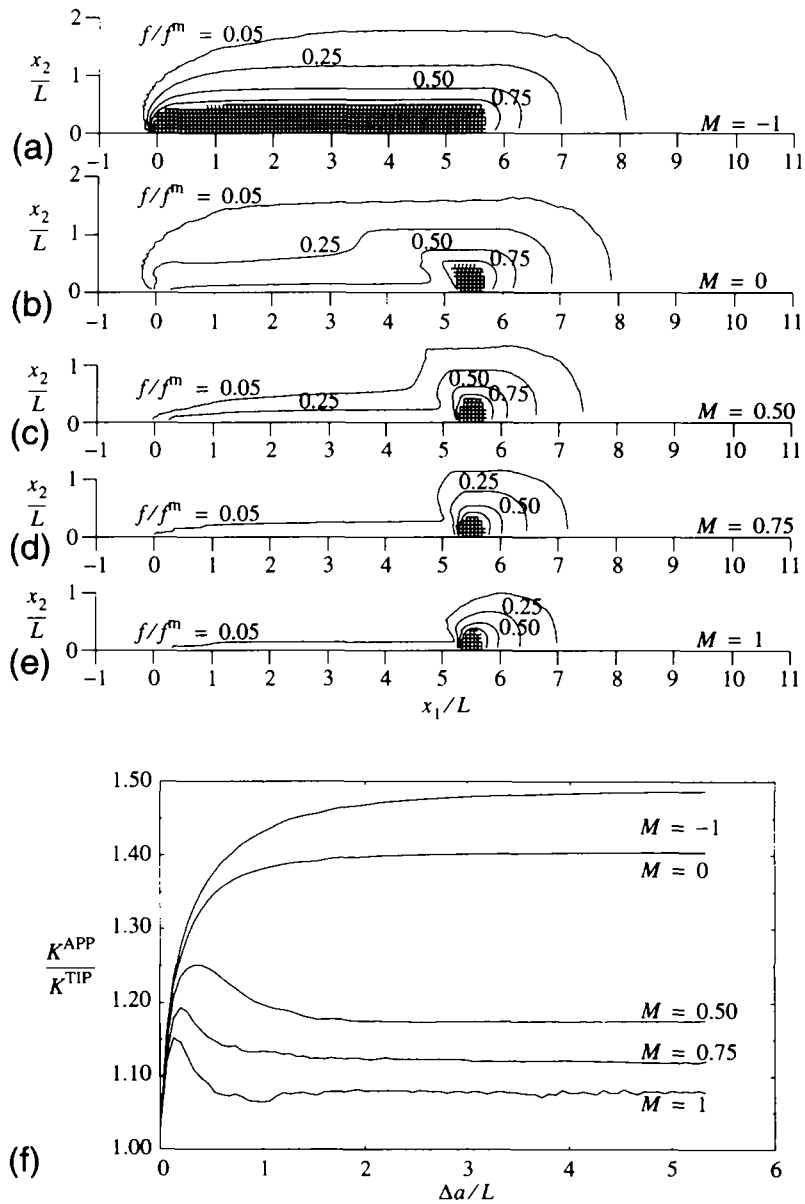

Fig. 6. Transformation zones (a–e) when $\Delta a = 5.33L$, and the crack growth resistance curve (f) for $\omega = 5$, $\alpha = 1.25$, $A = 0.045$ and $M = -1$ to 1.

shown. Note that in this case we use ω' instead of ω. We computed results for $\omega' = 5$ and $\omega' = 20$.

To check the convergence of the solution, some computations with refined meshes have been performed. In this small-scale problem, mesh refinement can be obtained simply by increasing the characteristic length L with respect to the dimensions of the smallest element, while leaving all other parameters unchanged. In this way the transformation zone will contain more elements

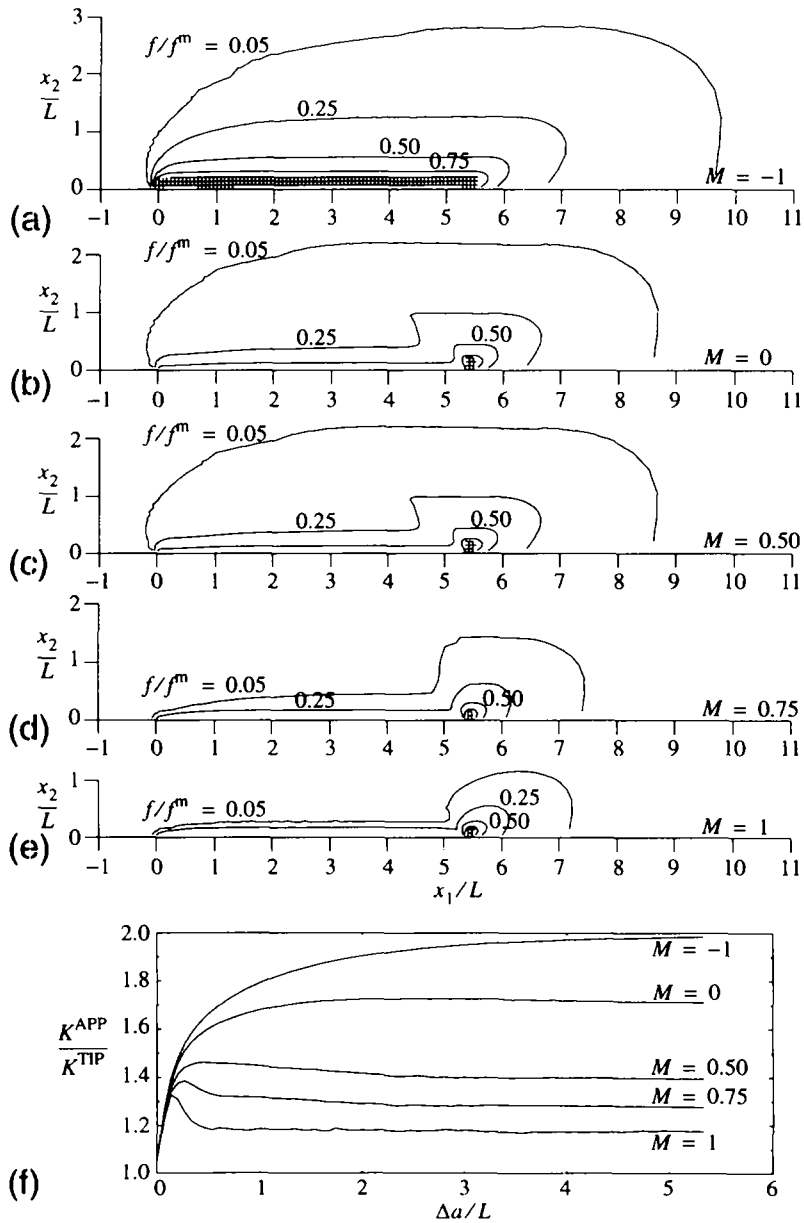

Fig. 7. Transformation zones (a–e) when $\Delta a = 5.33L$, and the crack growth resistance curve (f) for $\omega = 10$, $\alpha = 1.15$, $A = 0.056$ and $M = -1$ to 1.

and more accurate results should be obtained, as long as the small scale condition is not violated. A typical crack growth computation up to a steady state situation required about 100 CPU hours on a SUN Sparc station 1.

4.1. Transformation zones

We visualize the size and the shape of the distribution of the transformed material surrounding the crack tip by means of contours of

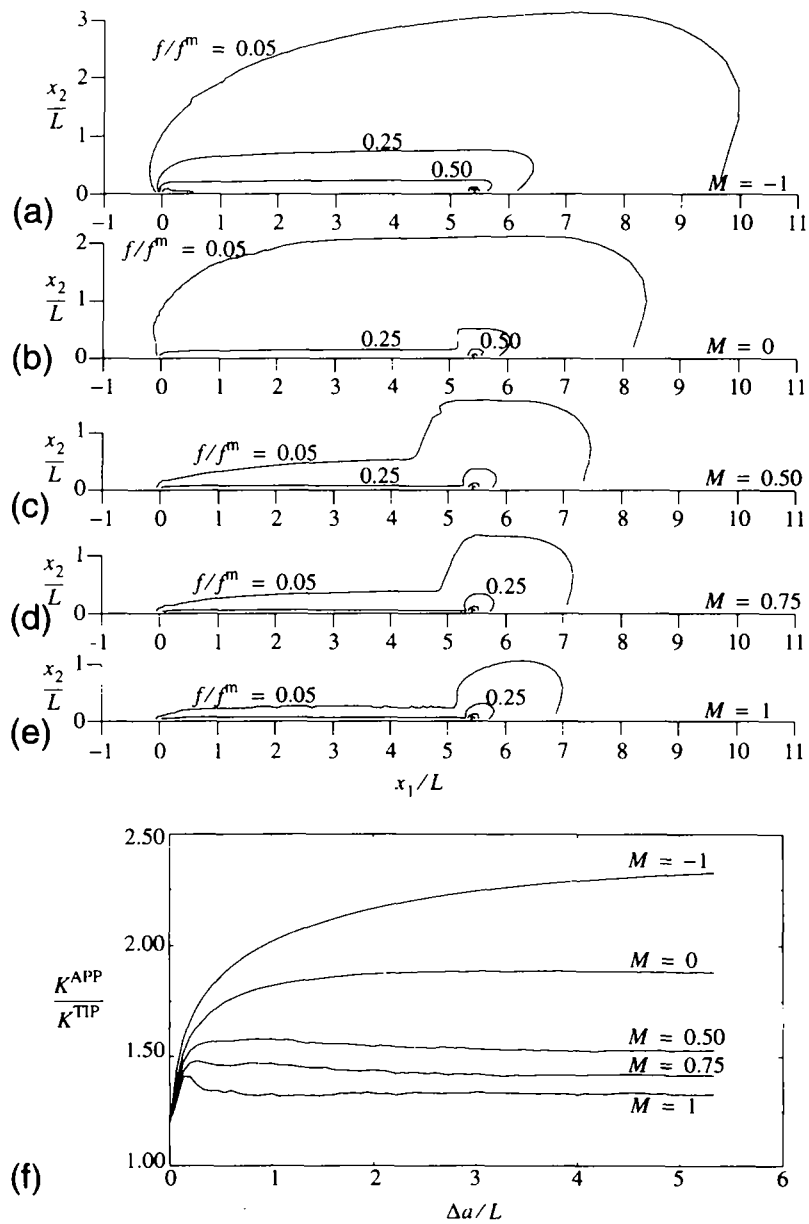

Fig. 8. Transformation zones (a–e) when $\Delta a = 5.33L$, and the crack growth resistance curve (f) for $\omega = 20$, $\alpha = 1.15$, $A = 0.056$ and $M = -1$ to 1.

constant ratio of transformed fraction to the maximum available fraction, f/f^m. Fully transformed material is high-lighted by plotting the boundaries of the elements which contain fully transformed material. The plots of the transformation zones are presented in Figs. 5–10.

As already explained in Section 3, the transformation is first triggered in the crack tip region.

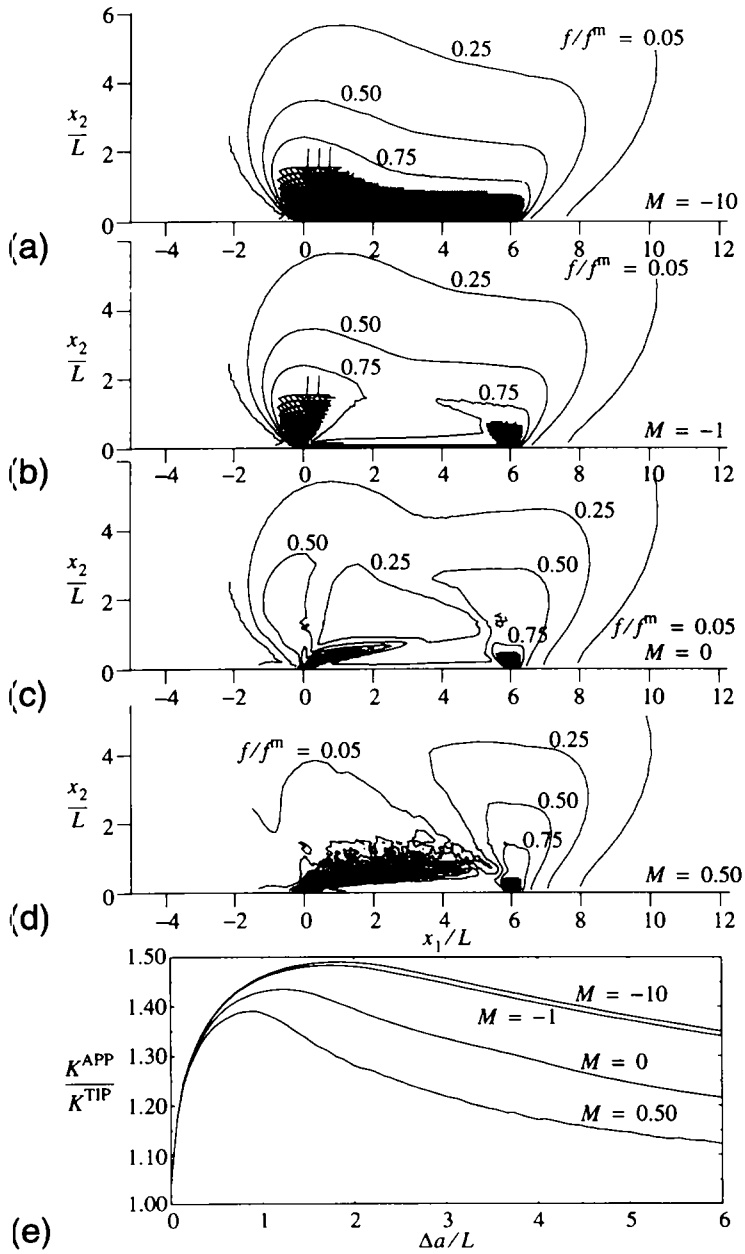

Fig. 9. Transformation zones (a–d) when $\Delta a = 6L$, and the crack growth resistance curve (e) for $\omega' = 5$ (purely shear transformations), $\alpha = 1.15$, and $M = -10$ to 0.50.

As the crack tip is approached from the frontal side, in general the amount of transformed fraction increases gradually up to the point where the material is fully transformed $f/f^m = 1$. The crack tip is usually surrounded by a fully transformed zone which itself is surrounded by a partially transformed zone, before the untransformed material is reached. Then, as the crack proceeds, the transformed material in the wake of the crack is exposed to unloading. This unloading may cause

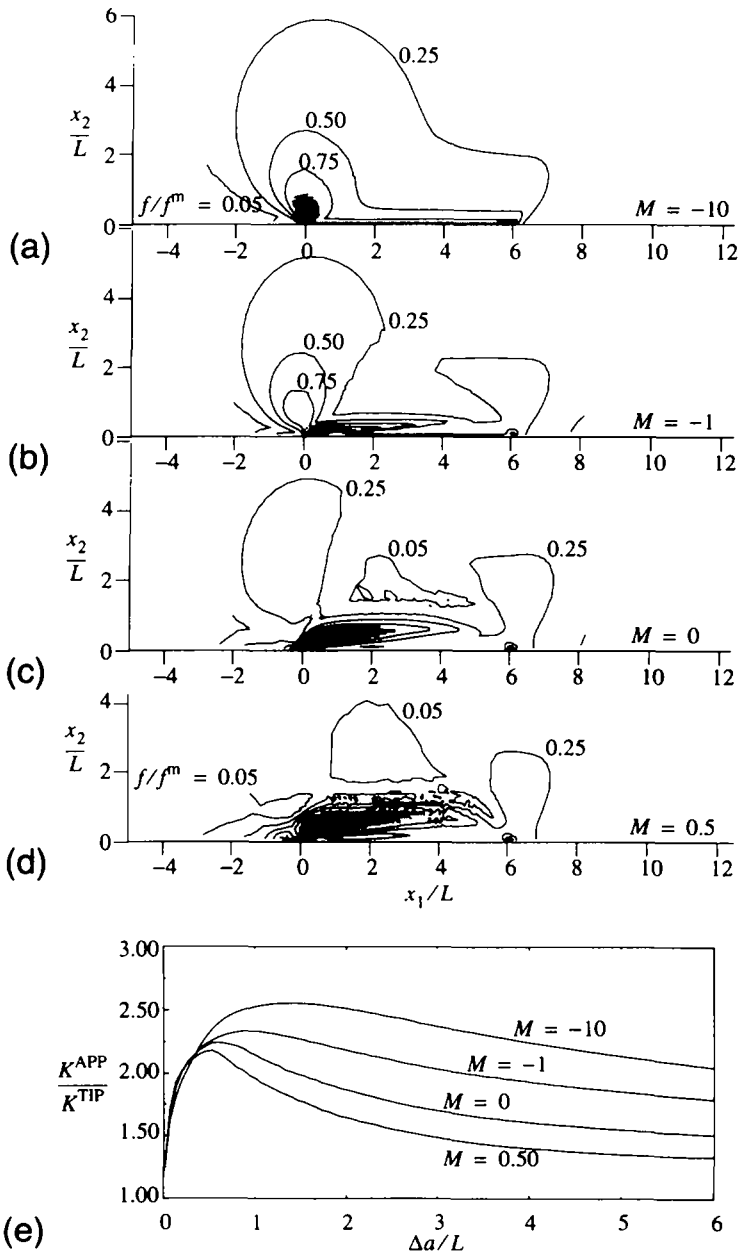

Fig. 10. Transformation zones (a–d) when $\Delta a = 6L$, and the crack growth resistance curve (e) for $\omega' = 20$ (purely shear transformations), $\alpha = 1.15$, and $M = -10$ to 0.50.

reverse transformation in this area. If the tendency to reverse transformation is very strong ($M = 1$) the material in the wake transforms back almost completely.

For transformations with dilatation and shear strains (Figs. 6–8), it is found that the volume of transformed material is always decreasing if reverse transformation occurs: reverse transformation does not trigger forward transformation anywhere else around the crack tip. In fact, the frontal zone hardly expands upon crack growth, which is usually the case if no reverse transformation occurs. In the latter case, the size of the frontal zone expands until a certain steady state value is reached. It may be said that for values of M larger than -1, reverse transformation occurs and the size of the frontal zone decreases. The effect of reversible transformation on the shape of the wake of the crack is, however, much more pronounced. When $M \geq 0$, the transformation strains in the wake of the crack are diminished rapidly. Two interesting phenomena can be noted when the amount of transformation shear strain A is varied. Firstly, for $M = 0$ and for $A = 0.0$, the wake of the crack is characterized by a sharp tail and the material in the wake near to the crack surface is fully untransformed (see the plot b of Fig. 5). For larger values of A, the shape of the transformation zone in the wake is changed drastically. In such cases the material near the crack surface remains transformed and the area further out is fully untransformed (see the plots b of Figs. 6, 7 and 8). Secondly, for dilatant transformation behavior, $A = 0$, and $M > 0$, extensive reverse transformation in the wake of the crack occurs, and the shape of the transformation zone is very similar to the shape of the transformation zone before the occurrence of crack growth: the so-called initial zone, which is shown in plots c, d and e of Fig. 5. For larger values of A, however, the shape of the transformation zone in the wake hardly changes. Only the remaining transformed area in the wake, near the crack surface, narrows down for M approaching 1 as shown in plots c, d and e of Figs. 6, 7 and 8.

For the more realistic values of the strength of the transformation, $\omega = 10$ and 20 shown in Figs. 7 and 8, respectively, we notice two pronounced differences with the results for $\omega = 5$. Firstly, the fully transformed areas are much smaller and, secondly, reversible transformation does occur even for $M = -1$. Reversible transformation for $M = -1$ occurs near the crack surface, where the unloading is most active.

The transformation zones for SMA show that reverse transformation for $M = -1$ always occurs as shown in plots b in Figs. 9 and 10. Therefore, computations for $M = -10$ have been performed to obtain results for the cases in which no material transforms back. The corresponding transformation zones are shown in plots a of the same figures and we see that the height of the transformation zone reaches a maximum before crack growth occurs. As soon as the crack starts growing, we see for $\omega' = 5$ that the height of the zone gradually decreases, while for $\omega' = 20$ the height is decreased more abruptly. For $M \geq -1$ it is observed that the initial zone (before crack growth) is rather stable and does not transform back easily. It is the transformation zone that develops upon crack extension which decreases considerably due to reverse transformation, as can be seen clearly in plots b and c of Figs. 9 and 10. For $M = 0.5$ the computations yield an irregular transformation zone. The stability of the computations becomes a problem: smaller load steps and an increased number of steps to release a node had to be taken. Computations for $M \geq 0.75$ failed; the numerical formulation appeared to be not accurate enough to deal with the fact that the forward (11) and backward (12) transformation surfaces are very close to each other.

4.2. Crack growth resistance

Prior to any crack growth it is reasonable to assume that no unloading occurs anywhere in the material. This was already stated by Budiansky et al. (1983). Therefore the starting value of the toughness has to be equal to the starting value for materials that do not show reverse transformation. For $A = 0$ (only dilatant transformation) the initial toughening due to the transformation strain is zero, but for $A > 0$ the initial transformation zone reduces the initial toughness: the transformation strains elevate the stress intensity near

the crack tip. Reverse transformation will only occur in the wake of the crack when the crack grows, and the material in the wake unloads.

The results for the parameter variations are given in the plots f of Figs. 5 to 8 and plots e of Figs. 9 and 10. From these plots we can see that the initial toughness is not affected by the value of M, as was to be expected. However, upon crack growth the amount of reversible toughness greatly influences the toughness development. The contribution of the transformation zone to the stress intensity at the crack tip may vary in between two extremes, namely

(i) the lower extreme of a vanishing contribution when all material in the wake transforms back,

(ii) when no material transforms back, the upper extreme for a certain parameter combination. In that case the toughness increase upon crack advance is found to be most pronounced.

In the latter case of irreversible transformations, the toughness tends to increase until a certain maximum value is reached, after which it decreases somewhat before settling on a steady state value. This is an effect that has first been observed by Stump and Budiansky (1989) for supercritical dilatant transformation behavior, and then by Hom and McMeeking (1990) also for subcritical transformations. Stam et al. (1994) have demonstrated this feature also for shear transformable materials, although for realistic material parameters the effects was not very profound.

In general we can conclude from Figs. 5–10 that if reverse transformation occurs immediately upon unloading ($M = 1$), the toughening effect reduces dramatically, which is most pronounced for dilatant transformations ($A = 0$), then no toughness increase is obtained at all. For $M = 1$, toughening is observed when $A > 0$, but only for crack extensions Δa up to about $0.4L$ and the maximum toughness increase is about 30% of the steady state toughness increase found in the absence of reverse transformation ($M \to -\infty$). After this peak value, the effect reduces rather rapidly to a value close to zero. Obviously, this peak behavior is of a different origin than that mentioned above for irreversible transformations. For the cases $M = 1$ and $A > 0$ it was found that more steps were needed to release nodes for the simulation of crack growth in order to maintain stability of the numerical calculation. Especially for $\omega = 5$, it must be noted that for the case $A = 0.045$ the number of unloading steps for the nodal release technique had to be increased 10 times to obtain reliable results. The same problem occurred for $M = 0.75$. For $M \leq 0.5$ no such problems have been encountered.

The effect of M on the toughness development for $A = 0$ is quite different from the effect for $A > 0$. For $A = 0$ in Fig. 5, no peak toughness is reached for the higher values of M, but the crack growth resistance increases monotonically to the steady state value. This steady state value steadily increases as the amount of reverse transformation decreases, i.e. M decreases. For $A > 0$ the toughness development for decreasing values of M is a transition of the curve for $M = 1$, with a maximum toughening effect after a crack extension $\Delta a \approx 0.4L$, to the curve for $M = -\infty$, where the maximum in toughness is reached much later and the drop in toughening after this maximum is far less severe. Note that for increasing values of ω, reverse transformation does occur for $M = -1$ and the toughening increase is reduced (see, e.g. Fig. 8). The maximum value of the toughness is found after a crack extension Δa of only L to $2L$, as shown in plots f of Figs. 9 and 10, for $M = -10$. When the value of M is increased we see that, similar to the previous results, the toughness increase upon crack growth decreases, but the decrease seems to be less severe.

Finally in Fig. 11 we show the spatial distribution of the toughness contribution due to the transformation strains (24) in terms of the value of $\mathrm{d}K^{\mathrm{TIP}}(\beta, r, E^{\mathrm{p}}_{\alpha\beta})$ normalized by K^{C}/L^2. Results are presented for each of the three types of transformation behavior defined in (21a)–(21c), after some crack growth, when a certain transformation zone has developed ($M = -10$ has been used to suppress reversal of the transformation). Budiansky et al. (1983) already showed that for dilatant transforming materials, the area ahead of the crack for $\beta < \pi/3$ (see Fig. 2) contributes negatively to the toughness increase while transformed material behind this line, in the wake of

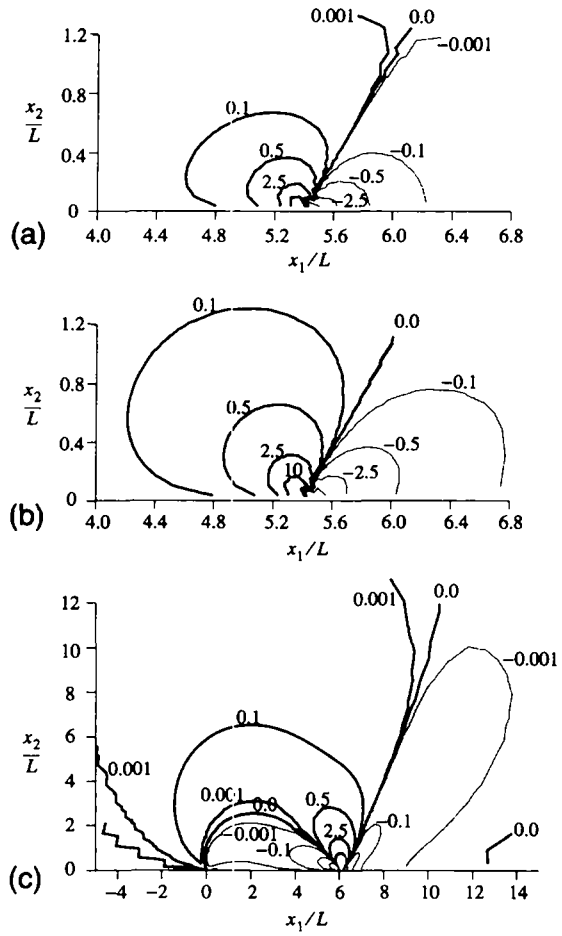

Fig. 11. The non-dimensional contribution to the toughness increase $dK^{TIP}\ L^2/K^C$ for $\nu = 0.3$, $\omega = \omega' = 20$, $\alpha = 1.15$ with (a) $A = 0$, $M = -10$, $\Delta a = 5.4L$, (b) $A = 0.056$, $M = -10$, $\Delta a = 5.4L$ and (c) $\varepsilon^{pd} = 0$, $M = -10$ and $\Delta a = 6.07L$.

the crack, increases the toughness. The change in sign at $\beta = \pi/3$ can be seen clearly in plot a of Fig. 11. We can see that the value of (24) in the region near the crack tip ($r < L/5$ approximately) is very pronounced. For materials with both shear and dilatation strains, we see a similar result: the area ahead of the crack tip ($\beta < \pi/3$) contributes negatively, while the transformation strains in the wake of the crack cause the toughening effect. However, for the transformation behavior with purely transformation shear strains, as shown in plot c, the results are different. Here we see that both the transformation strain in the wake close to the crack surface and the transformation strains ahead of the crack tip give a negative contribution. Close to the tip, the line at $\pi/3$ still represents the border between positive and negative contributions, but the border approaches $\beta = \pi/2.5$ for larger r.

5. Conclusions

This study clearly shows that transformation toughening during crack growth does depend strongly on the amount of reverse transformation. In all cases considered, the toughness increase upon crack growth is reduced if reverse transformation takes place in the wake of the growing crack. The decrease is most dramatic for so-called super- or pseudo-elastic materials ($M = 1$), where reverse transformation immediately follows upon unloading. It may be concluded from the parameter study, that this class of materials exhibits some initial toughening, but after a small amount of crack growth almost no toughness increase is left.

For ceramics containing zirconia there seems to be no direct experimental evidence for reverse transformation at room temperature in simple tensile tests. Even though there is some experimental evidence for reverse transformations taking place under compression at room temperature (Subhash and Nemat-Nasser, 1993), the amount of reversal upon unloading is rather limited. Hence, these materials seem to be characterized by $M < 0$, for which our results show that the reduction in toughness increase is not so dramatic. However, further experimental work is necessary to establish the actual value of M as the influence of this parameter on the crack growth resistance is substantial. Although the toughness increase is always reduced when the transformation is reversible, it is reassuring that even for pseudoelastic materials ($M = 1$) not all toughness increase upon crack growth is lost.

For dilatant supercritically transforming materials, where the transformation occurs instantaneously and completely (as analyzed by Budiansky et al. (1983); see also Section 2.2), the effect

of reverse transformation on the toughening has been estimated by Evans and Cannon (1986). They found that, when forward transformation occurs at some critical mean stress Σ_m^C and reverse transformation occurs at another critical mean stress $\Sigma_m^R \geq 0$, the toughening increase is

$$\Delta K^{TIP} = -0.21 \frac{3E\varepsilon^{pd} h^{1/2}(1 - \Sigma_m^R/\Sigma_m^C)}{(1-\nu)}, \quad (29)$$

where h is the half-height of the transformation zone. Consequently when the transformation reverses to give zero final stress ($\Sigma_m^R = 0$), the toughening value is identical to the estimated value for the supercritical, unreversed case given by McMeeking and Evans (1982), and is zero when $\Sigma_m^R = \Sigma_m^C$. In our terminology the latter case would refer to $M = 1$, and the zero result for the increase in toughness agrees with the subcritical results presented here for $A = 0$. The other extreme, when the transformation-induced dilatation is zero, has been considered by Sun and Xu (1993) for SMA materials in the pseudoelastic range. However, the practical value of their analysis may be questioned, as we found that the shape of the transformation zone is heavily affected by the transformation strains itself; this effect has not been accounted for in their analysis.

For SMA the toughening effect due to phase transformations has been found to be substantially higher than for ceramics, for the same values of the respective strength parameters ω' and ω. Care should be exercised, however, in relating the present results to real SMAs, since the present constitutive model may account only partially for all mechanisms involved. For instance, the present model does not account for dislocation plasticity that may accompany fracture in some real SMA materials, nor for ductile failure mechanisms involving void growth and coalescence. On the other hand, some experimental evidence for toughening caused by the martensitic transformation in brittle SMA has been reported by McNichols et al. (1981) and by Murthy and Goo (1992). Yet for quantitative conclusions, better estimates of the material parameters are needed.

References

Amazigo, J.C. and B. Budiansky (1988), Steady-state crack growth in supercitically transforming materials, *Int. J. Solids Struct. 24*, 751.

Bowman, K.J., P.E. Reyes-Morel and I.-W. Chen (1987), in: *Material Research Society Symposium Proceedings*, Vol. 78, Eds. P.F. Becher, M.V. Swain and S. Somiya, p. 51.

Budiansky, B., J.W. Hutchinson and J.C. Lambropoulos (1983), Continuum theory of dilatant transformation toughening in ceramics, *Int. J. Solids Struct. 19*, 337.

Chen, I.-W. and P.E. Reyes-Morel (1986), Implications of transformation plasticity in zirconia-containing ceramics: I. Shear and Dilatation effects, *J. Am. Ceram. Soc. 69*, 181.

Chen, I.-W. and P.E. Reyes-Morel (1987), in: *Material Research Society Symposium Proceedings*, vol. 78 Eds. by P.F. Becher, M.V. Swain and S. Somiya p. 75.

Deleay, L., R.V. Krishnan, H. Tas and H. Warlimont (1974), Review – Thermoelasticity, pseudoelasticity and the memory effects associated with martensitic transformations, Part I: Structural and microstructural changes associated with the transformations, *J. Mat. Sci. 9*, 1521.

Eshelby, J.D. (1961), Elastic inclusions and inhomogeneities, in: *Progress in Solid Mechanics II*, Eds I.N. Sneddon and R. Hill, North-Holland Publishing Company, Amsterdam, pp. 89.

Evans, A.G. and A.H. Heuer (1980), Transformation toughening in ceramics: martensitic transformations in crack-tip stress fields, *J. Am. Ceram. Soc. 63*, 241.

Evans, A.G. and R.M. Cannon (1986), Toughening of brittle solids by martensitic transformations, *Acta Metall. 34*, 761.

Fischer, F.D., M. Berveiller, K. Tanaka and E.R. Oberaigner (1994), Continuum mechanical aspects of phase transformations in solids, *Arch. Appl. Mech. 64*, 54.

Hom, C.L. and R.M. McMeeking (1990), Numerical results for transformation toughening in ceramics, *Int. J. Solids Struct. 26*, 1211.

Hutchinson, J.W. (1974), *On Steady Quasi-static Crack Growth*, Harvard University Report TR74-1042.

Krishnan, R.V., L. Deleay, H. Tas and H. Warlimont (1974), Review – Thermoelasticity, pseudoelasticity and the memory effects associated with martensitic transformations, Part II: The macroscopic mechanical Behavior, *J. Mat. Sci. 9*, 1536.

Lambropoulos, J.C. (1986), Shear, shape and orientation effects in transformation toughening, *Int. J. Solids Struct. 22*, 1083.

Marshall, D.B. and M.R. James (1986), Reversible stress-induced martensitic transformation in ZrO_2, *J. Am. Ceram. Soc. 69*, 215.

McMeeking, R.M. and A.G. Evans, (1982), Mechanics of transformation-toughening in brittle materials, *J. Am. Ceram. Soc. 65*, 242.

McNichols Jr, J.L., P.C. Brooks and J.S. Cory (1981), NiTi fatigue behavior, *J. Appl. Phys. 52*, 7442–7444.

Mori, T. and K. Tanaka (1973), Average stress in matrix and average elastic energy of materials with misfitting inclusions, *Acta Metall. 21*, 571.

Murthy, A.S. and E. Goo, (1992), Study of transformation-induced ductily in polycrystalline nickel aluminide, *Materials Research Society Symposium Proceedings*, Vol. 246, pp 129–134.

Otsuka, K. and K. Shimizu (1986), Pseudoelasticity and shape memory effects in alloys, *Int. Met. Rev. 31*, 93.

Patoor, E., A. Eberhardt and M. Berveiller (1987), Potentièl pseudoélastique et plasticité de transformation martensitique dans les mono- et polycristaux metalliques (in French), *Acta Metall. 35*, 2779.

Reyes-Morel, P.E. and I.-W. Chen (1988), Transformation plasticity of CeO_2-stabilized tetragonal polycrystals: I. Stress assistance and autocatalysis, *J. Am. Ceram. Soc. 71*, 343.

Reyes-Morel, P.E., J.S. Cherng and I.-W. Chen (1988), Transformation plasticity of CeO_2-stabilized tetragonal polycrystals: II. Pseudoelasticity and shape memory effect, *J. Am. Ceram. Soc. 71*, 648.

Sano, Y., S.N. Chang. M.A. Meyers and S. Nemat-Nasser (1992), Identification of stress-induced nucleation sites for martensite in Fe–31.8wt% Ni–0.02wt% C alloy, *Acta Metall. Mater. 40*, 413.

Stam, G.Th.M. (1994), *A Micromechanical Approach to Transformation Toughening in Ceramics*, Ph.D. thesis, Delft Univ. of Technology.

Stam, G.Th.M. and E. Van der Giessen, (1994), Analysis of the effect of transformation-induced shear strains on stability and crack growth in zirconia-containing ceramics, in: *Fracture Mechanics*: 25th volume, ASTM STP 1220, Eds. F. Erdogan and R.J. Hartranft, Philadelphia, USA, to appear.

Stam, G.Th.M. and E. Van der Giessen (1993), Analysis of the effect of reversible transformations on the toughness of ceramics, *Proc. Plasticity '93*, ed. A.S. Kahn, Baltimore, USA.

Stam, G.Th.M., E. Van der Giessen and P. Meijers (1994), Effect of transformation-induced shear strains on crack growth in zirconia-containing ceramics, *Int. J. Solids Struct. 31*, 1923.

Stump, D. and B. Budiansky (1989), Crack-growth resistance in transformation-toughened ceramics, *Int. J. Solids Struct. 25*, 635.

Subhash, G. and S. Nemat-Nasser (1993), Dynamic stress-induced transformation and texture formation in uniaxial compression of zirconia ceramics *J. Am. Ceram. Soc. 76*, 153.

Sun, Q.P. and K.C. Hwang (1993a), Micromechanics modelling for the constitutive behavior of polycrystalline shape memory Alloys – I. Derivation of general relations, *J. Mech. Phys. Solids 41*, 1.

Sun, Q.P. and K.C. Hwang (1993b), Micromechanics modelling for the constitutive behavior of polycrystalline shape memory alloys – II. Study of the individual phenomena, *J. Mech. Phys. Solids 41*, 19.

Sun, Q.P. and X.J. Xu (1993), On the pseudoelastic toughening of shock-resistant composite with transformable reinforcement submitted to *Mech. Mater.*

Sun, Q.P., K.C. Hwang and S.U. Yu (1991), A micromechanics constitutive model of transformation plasticity with shear and dilatation effect, *J. Mech. Phys. Solids 39*, 507.

Warlimont, H., L., Deleay, R.V. Krishnan and H. Tas, (1974), Review – Thermoelasticity, pseudoelasticity and the memory effects associated with martensitic transformations, Part III: Thermodynamics and kinetics, *J. Mat. Sci. 9*, 1545.

Zhang, J.M. and K.Y. Lam (1994), Transformation shear of precipitated ZrO_2 particles in the presence of multi-mode twinning, *Int. J. Solids Struct. 31*, 517.